

DOI 10.14622/Advances_48_2022_07

Evaluation of measurement methods for compression, re-swelling and material thickness through the embossing process of cardboard

*Ulrike Kaeppler^{1,2}, Jennes Huenniger^{1,2} and Lutz Engisch^{1,2}*¹ Leipzig University of Applied Science, Faculty of Media and information Science, Karl-Liebknecht-Str. 132, 04277 Leipzig² iP³ Leipzig – Institute for Printing, Processing and Packaging Leipzig, Karl-Liebknecht-Str. 132, 04277 Leipzig

E-mail: ulrike.kaeppler@htwk-leipzig.de

Short abstract

The subject of the present study is the detection and measurement of the material thickness after embossing, the compressibility and the re-swelling on embossed board samples using various methods. Knowledge of these aspects is relevant for the production of high-quality embossed structures. One aspect is to achieve the highest possible deformation in the process, with little shrinkage even after the samples were pressure relieved. In addition to the forming effect, densification and the degree of re-swelling also play a decisive role in the quality of the product. Furthermore, it is important to gain such an understanding of the material in order to be able to model the material in FEM simulations. Studies on the forming behavior of paper and board are well known from the field of deep drawing. These experimental studies mainly look at the wrinkle distribution in the product. Other researchers have not yet found out which is the best method to analyze the thickness of the material after the sample has been relieved of force in order to obtain efficient and reliable results. Therefore, this study focuses on finding a suitable analysis method to detect material compaction and thus measure the different material thicknesses of embossed paperboard samples. In order to validate different analytical methods, they need to be tested experimentally. In addition, the results are related to the compressibility and the re-swelling after deflating the material. It was found that the material thickness within the embossing geometry can be measured most efficiently with a digital cross section. Furthermore, it can be assumed that the re-swelling is related to the degree of forming. So far, the compressibility in the embossing gap still differs from that of the single measurement.

Keywords: embossing, material compression, re-swelling

1. Introduction

1.1 Material

Embossing is used as optical and haptical effect for packaging such as cardboard folding boxes. For example, the embossing highlights a logo on folding boxes or braille letters on medical products. Embossing is an important part of print finishing. Especially with regard to the sustainability debate, embossing is a very sustainable finishing process without the use of additional raw materials such as foils, varnishes, etc.

Paper and cardboard are single- or multilayer fiber composites. Fibers generally consist of three main components: 40 % cellulose, 30 % hemicellulose and 20 % to 30 % lignin (Bayerl and Pichol, 1986; Ek, Gellerstedt and Henriksson, 2009).

These multiple layers of cardboard are not glued. The fibers are only linked together by intermolecular forces in form of hydrogen bonds (Radzanowski, 2017; Brenner, 2016).

The layers may have the same or varying compositions. Thus, it is one of the important aspects of material properties besides the bonding within the layers as well as the fibers (Blechsmidt, 2013). Because of this, different materials show different mechanical behavior during forming.

1.2 Process

During the embossing process, the material is shaped between the male and the female die. First, the roughness peaks of the fiber composite are equalized (Schaffrath and Göttsching, 1992). Then the compression of the fibers as well as the eliminations of hole structures follows until the complete compaction of the material. The pore volume decreases close to zero (Hauptmann, 2013).

The embossing process stretches the material. This is due to the fact that the projected area is always larger than the initial area, depending on the embossing height. Initially, the material withstands the stretching. Especially on the outside of the embossing, the impact of stretching is very high. In addition, there are many material tensions which are indicated by an uneven base surface after embossing. If the material is stretched too much, it cracks. Fibers remain connected via hydrogen bonds, but those forces decrease with increasing distance. If the material is stretched too much, the distance increases and the fiber structure breaks.

There are studies on deep drawing of cardboard but the analysis is focused on the wrinkle distribution. The differences between deep drawing and embossing are the lack of a blank holder in embossing, the dimensions are different and folding is undesirable in embossing (Meyer, 2015; Oehm, 2010; Wallmeier, 2018; Weber, 2017). To analyze crack formation during embossing, different methods of analysis such as coloring with safranin and with carbon, embedding and cross sections are examined.

The quality of the embossing depends among other things on the degree of shaping. Too little shaping leads to blurred contours. As the embossing path increases, the material becomes more compressed and the material thickness in the flanks get smaller. Too much shaping, though, leads to crack formation. These cracks are unwanted because they interfere with the appearance of the embossed product.

1.3 Compression and compression areas

During material forming, the cardboard is compressed between the male and female die. The remaining gap between the two tools determine the maximum material thickness at each embossing path. The more embossing path covered, the less gap is between the tools. If the distance between the tools falls below the material thickness in the initial state, the material is inevitably compressed. The degree of compressibility is material-specific.

In order to analyze different compression areas distributed over one embossing geometry, the test geometry truncated pyramid has proven to be useful. Due to the geometric conditions, the truncated pyramid can be divided into three areas of interest: Outer area, flank area, top area. Within the area, further parameters can be defined, which are described in chapter 2.3.

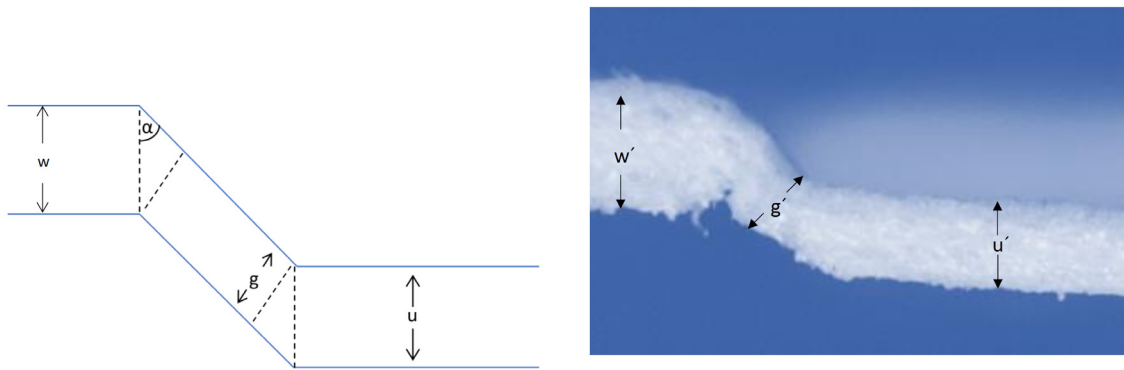


Figure 1: Measurement of material thickness at different compression areas

Figure 1 shows a cross section of an embossed cardboard. Three parameters describe the material thickness in each of the three areas.

w: Area outside the embossing geometry

g: Area within the flank of the embossing geometry

u: Area in top of the embossing geometry

From various specifications of tool, material and embossing path, the gap distances can be calculated according to Equations [1] and [2].

$$u = \text{Element height} - (\text{Embossing path} - \text{Material thickness}) \quad [1]$$

$$g = \sin(\alpha) * u \quad [2]$$

The stress-strain behavior of paper and board in the tensile test shows that elastic and subsequent plastic deformation takes place until failure (Hauptmann, 2013). In case of the compression, the viscoelastic component has to be taken into account as well. Due to the re-swelling, the deformation of the material under load differs from the subsequent state after load release of the embossed sample.

1.4 Research questions

The resulting material thickness from the shaping processes has not been analyzed in depth so far. Knowledge of the distribution of material thickness within an embossing geometry is important for the understanding of the material behavior during the process. The material is formed three-dimensionally and compressed. The compression does not take place equally at all points. The material thickness is a characteristic value for the quality of the representation of the interaction properties, especially for the understanding of re-swelling processes.

A measurement of the material thickness according to DIN EN ISO 534 is obsolete for three-dimensional formed materials (Deutsches Institut für Normung, 2011). Three-dimensional shaping results in flanks, i.e. areas that are not parallel to the actual original cardboard grade. Thus, the measuring device should either have to be mounted at right angles to the surface of the flanks or this should be taken into account within the measuring analysis. Figure 2 shows the different measured values for measurements at right angles to the zero line and at right angles to the material surface. The gray sketch is the embossed material (truncated pyramid).

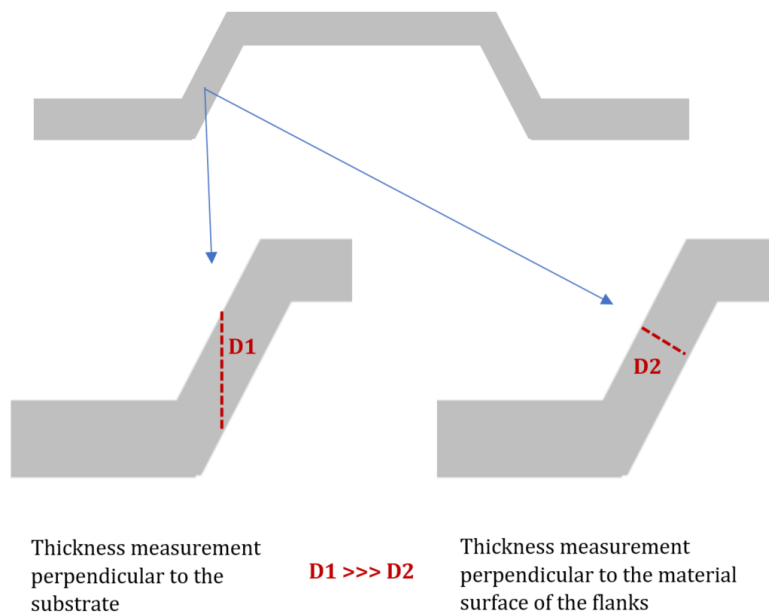


Figure 2: Comparison of the material thickness measurements in relation to the surface of the zero line and the material surface

1.5 Existing studies on the measurement of the material thickness of the embossed board sample after the embossing process after load release

There are some approaches for determining the material thickness of fiber composite materials. In a former study, the samples were placed between two pieces of metal and foam rubber and fixated with a Hofmann screw clamp. This clamp has two plano-parallel elements that can be shifted against each other. Thus, they are good to fix the sample in place. The rubber avoids the compression of the material due to internal forces (see Figure 3).

A sharp razor blade was used to create an almost artefact-free cross-section of the sample (Käppeler, 2019; Schuhmann, Hodes and Engisch, 2016). For this method it is not analyzed yet, if the samples get damaged through cutting. If so, for example, the measured material thickness by fanning out the sample could be higher than the real sample thickness.

In addition, another method known from botanical objects and microtome examinations was used. The samples were embedded in a block of different natural or synthetical resins or paraffin waxes (Schrödel, 2011; Scheuter, 1980). Schuhmann, Hodes and Engisch analyzed printed paper and used methacrylate- and epoxy-resins to prepare the samples. The paper samples were put in a hexagonal container. The samples were embedded in the resins and hardened by ultraviolet radiation. Afterwards, the block was fixed into a microtome cutter to produce thin microtome cuts (Schuhmann, Hodes and Engisch, 2016).

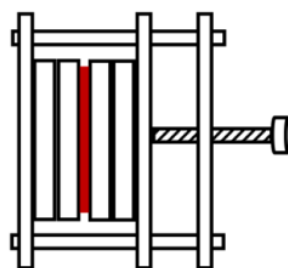


Figure 3: Method of the Hoffman screw clamp for preparing the cross sections (Käppeler, et al. 2020)

This method is quite laborious and time-consuming due to the small-scale embedding process. In addition, there is a high risk that the sample is not ideally vertical in the embedding or shift during the sample preparation. Then the sample would not be cut exactly perpendicular to the plane. Furthermore, it cannot be clarified whether the resins have an influence on the forming, for example due to penetration into the sample.

In both analytical methods, the material thicknesses of the samples would be measured with a microscope.

2. Materials and methods

2.1 Materials and embossing process

Cardboard is a typical material for folding boxes used for packaging products. The examined cardboard has three layers made from fibers. The three types of cardboard used are shown in Figure 4.

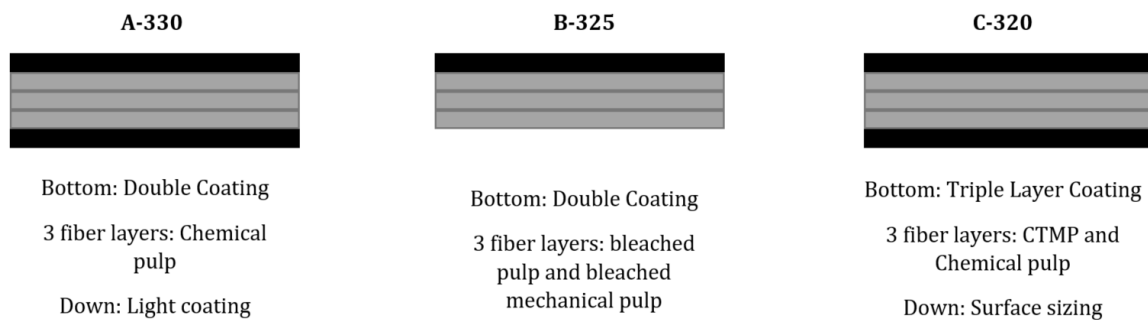


Figure 4: Three different types of cardboard used

The material thickness in the initial state is measured with a Frank thickness device (FRANK-PTI GmbH, Birkenau, Germany) according to DIN EN ISO 534. 10 samples per cardboard type are measured and the mean is reported with two-sided confidence interval ($\alpha = 5\%$, t -distribution).

A truncated pyramid is used as embossing geometry. The edge length of the truncated pyramid is 5 mm. The angles are 45° and the height is approximately $620\ \mu\text{m}$. The geometry is shown in Figure 5. Due to the dimensions and angles, the geometry is designated with the abbreviation PS45-5.

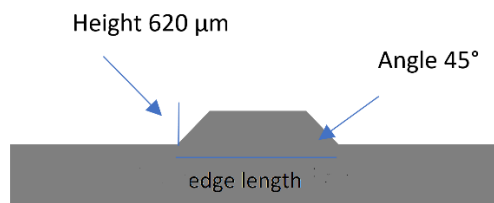


Figure 5: Schematic dimensions of the embossing geometry (PS45-5)

In the process, the embossing tools are moved into each other by two guided parallel tools. The material in between is pushed into the mold, where it is shaped and pressed (see Figure 6). The process ends when no change of the embossing path is longer detected while the force still increases. The experiments were carried out with a Tensile-Compression Testing- Machine (Zwick Roell, Ulm, Germany).



Figure 6: Schematic representation of the embossing process (flat embossing, relief embossing) – left side: wide spacing of the embossing tools, no material contact; middle: first material contact without shaping; right: material shaping, embossing tools move into each other

2.2 Compression behavior

The approaches were carried out on three different cardboards shown in Figure 4. The thickness of the samples was measured in the initial state according to DIN EN ISO 534. The samples were subsequently compressed in a compression test rig (Käppeler, et al, 2022). This was used to determine the compressibility of the material under maximum load.

The three materials were compressed. From the geometric considerations it can be seen that compression of the material occurs during the embossing test, particularly in the flanks of the truncated pyramid. At the end of the process, the distance between the flanks is less than the actual material thickness; consequently, the material must have been compressed. The end of the process is reached when the compression force increases exponentially, but almost no more increase in the embossing path can be observed. This process end differs from carton type to carton type. A correlation between material compressibility, distance in the embossing gap of the flanks and process end is still to be found.

The compression behavior of the material is determined by an equivalent test. For this purpose, a circular punch with a diameter of 10 mm is pressed into the material against a plane-parallel plate. It is measured how far and with how much force the punch can be pressed into the material. The compression process ends when the material is completely compressed. Complete compression is shown in the path–force–diagram by an exponentially increasing force with hardly any increasing compression displacement.

After compression is completed, the sample is relieved. The material in the relieved state swells back. This means that the compressing depth in the relieved state is lower than pressure relieved. Therefore, the compressed contours in the relieved state are less pronounced, i.e. less sharp and rich in contours, than in the loaded state within the process. This is measured by imaging the sample with a Keyence 3D VR-3000 Macroscope (Keyence, Neu-Isenburg, Germany) stripe light macroscope. In the virtual cross-section through the sample, the resulting compression indentation depth is determined.

2.3 Compression areas within the embossing process

A scale sketch was created to gain a better understanding of the process. Figure 7 shows the male and the female die as well as the material in between. The sketch shows the end of the process, i.e. when the forming end is reached. The shaded sections show the areas where the material is compressed. The compression range depends on the material and its specific compressibility. The material is compressed in the top area, but especially in the flanks.

The following characteristic values are measured:

- (1) The embossing path: The distance covered by the machine from the start time, when the pre-force is reached until the maximum force is reached.
- (2) Tool gap flank: The distance between the male and the female die in the area of the flanks.
- (3) Tool gap inside: The distance between the male and the female die in the area of the top.
- (4) Material thickness: The original material thickness of the board without forming.

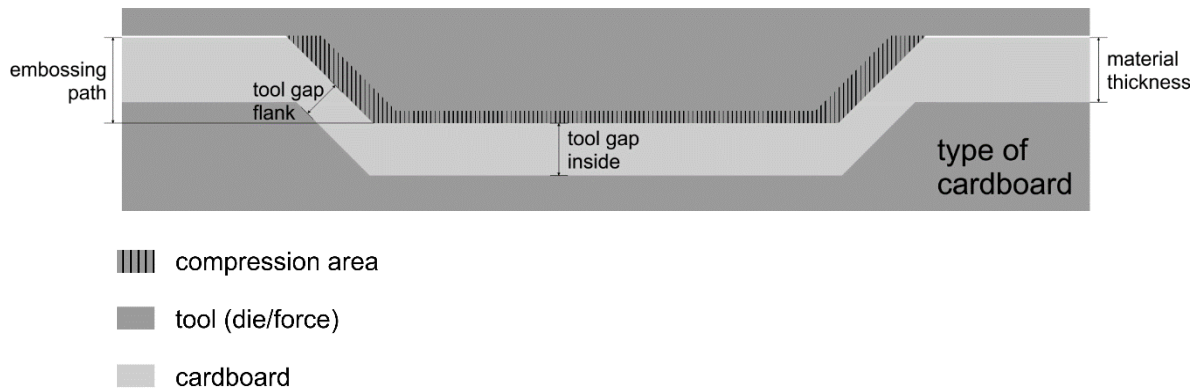


Figure 7: Effect Pairing analysis for calculating the material thickness under load (Hünniger, 2020)

2.4 Material re-swelling

A test method was developed for investigating the re-swelling behavior of the board materials. The process is shown in Figure 8. For this purpose, the compression test tool is pressed into the material. The force and the associated compression path are detected. The resulting impression is recorded with a Keyence VR-3000 macroscope (Keyence, Neu-Isenburg, Germany). A virtual cross-section is placed in the center of the circular indentation and the remaining indentation depth is measured.

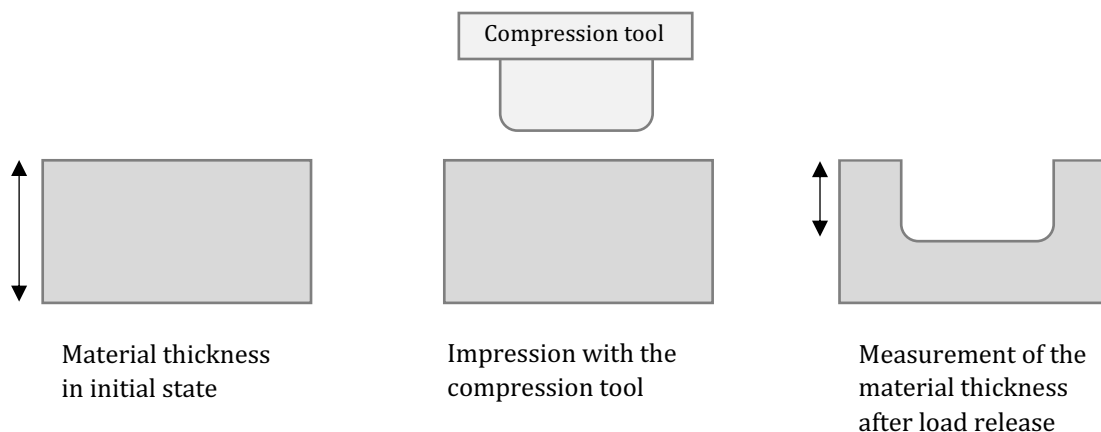


Figure 8: Test sequence for measuring the indentation depth after compression of the material

2.5 Methodology for determining the material thickness of embossed samples after load release

2.5.1 Real cross sections

Cross-sections are to be created in order to measure the material thicknesses in the material cross-section. Similar to the described sample cutting with the hose clamps, the samples were cut by using a cutting mat and a sharp razor blade (Figure 9). The results of these two cutting methods do not differ significantly. Therefore, the cutting method without any clamps was used for the following experiments.

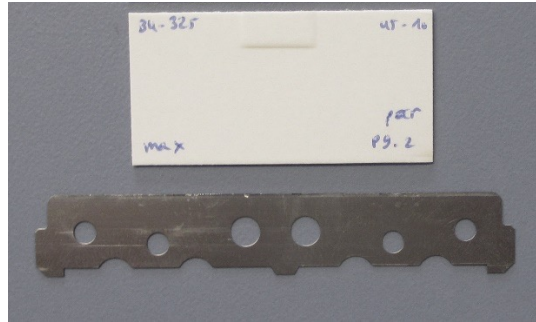


Figure 9: Sharp razor blade for making cuts without clamping

The cross-sections were examined with a macroscope measurement device Keyence VR-3000 (Keyence Deutschland GmbH, Neu-Isenburg, Germany). The measurement technique is stripe light projection which can be used to create three-dimensional surface scans. The material thickness of the samples was detected at the cross-section of the embossed samples.

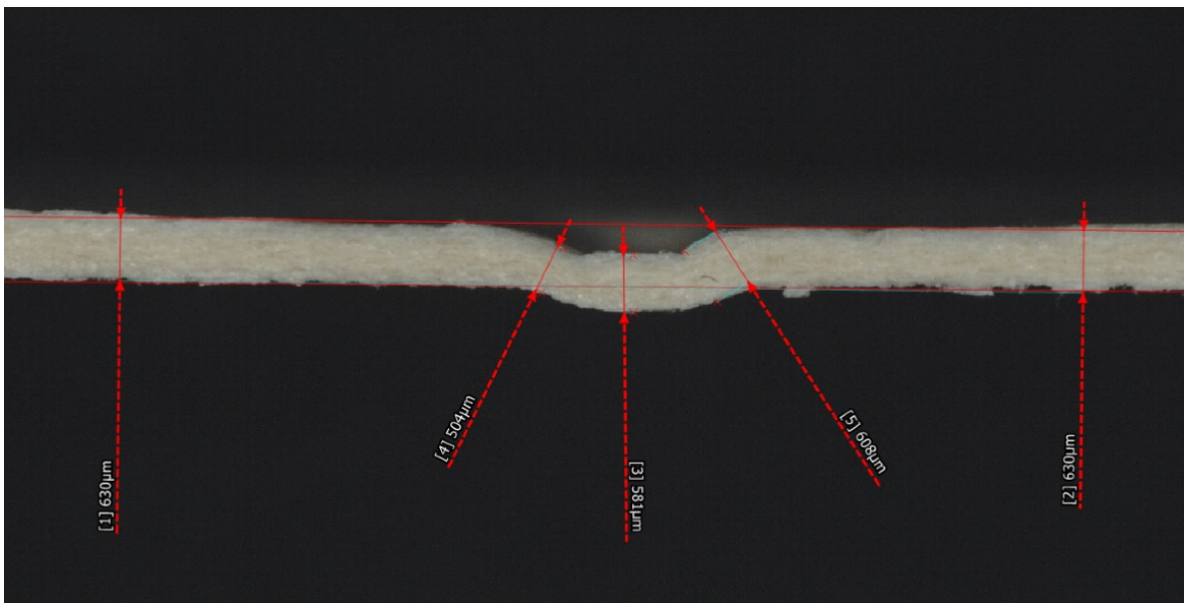


Figure 10: Measurement of material thickness in cross section with embossing geometry PS45-5

Figure 10 shows the results of a measured sample. The positions [1] and [2] were not compressed during the embossing process, because they are located outside the embossing element and therefore present the original material thickness. The positions [3] in the center and [4]; [5] in the flank areas were compressed during the embossing process and show the compressed areas after load release of the sample.

2.5.2 Virtual cross section

To combine the measurement results of the upper and the bottom side of embossed samples, the analysis tool “Measurement Comparison” is used. The device detects the surface topographies of the samples (Figure 11, left) and the data is visualized as a 3D-plot (Figure 11, middle).

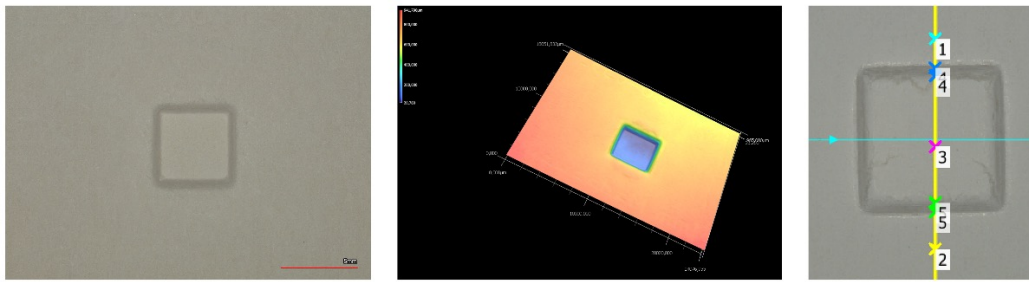


Figure 11: Measured 3D-topography of the samples and the virtual cross sections placed in the middle of the sample

The measurement data of the upper and the bottom side are positioned relative to each other so that the measured material thickness of the cross-section analysis (Figure 11) is achieved outside the embossing element (Figure 12).

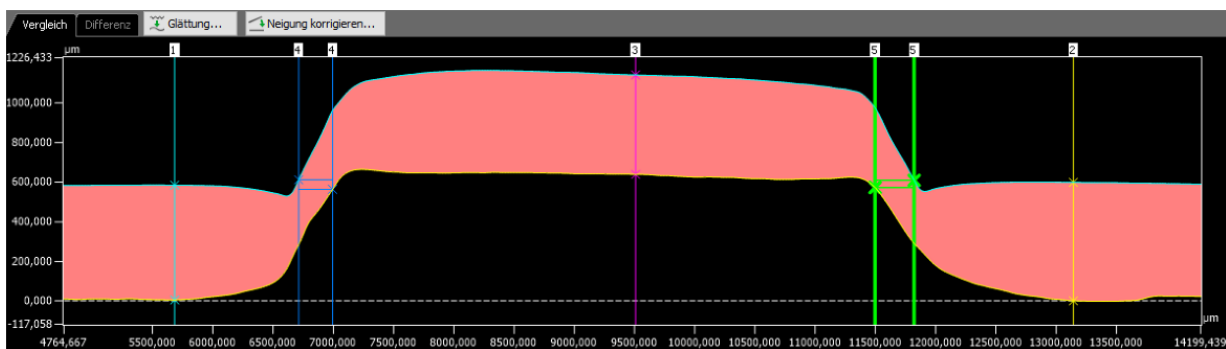


Figure 12: Digital measurement comparison for determining the material thickness of an embossed cardboard sample (PS45-5)

To calculate the material thickness in the embossing area, the cross-sections were put above each other with a definite gap (Figure 12, point 1). This gap was considered as a region far off the embossing area where no deformation took place. Thus, it represents the original thickness of the sample. All the other gap sizes between the upper and the bottom sample cross section were related to that present gap size. Besides the original material thickness (Figure 12, points 1 and 2), the thickness of the middle of the element (Figure 12, point 3) as well as of the flanks (Figure 12, points 4 and 5) were measured.

2.5.3 CT-cross section

Another method is the analysis of the compression with computer tomography (CT) measurements.

The following CT-parameters were chosen: 1 800 pictures, 4 ms measuring time for one shot, temperature 23 °C, current 120 ampere, power 80 volt, 4.8 µm voxel size. Figure 13 shows a cross-section within the embossing geometry of several samples. The samples were all of the same material; they just differ in the chosen embossing paths.

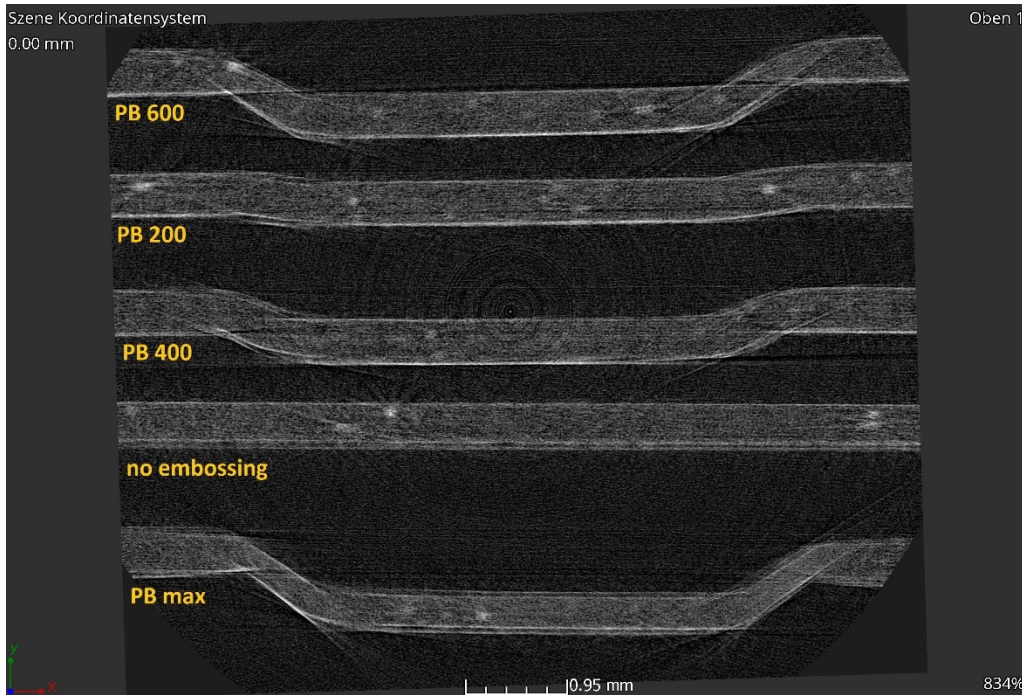


Figure 13: X-ray CT measurement of embossed board samples with different embossing paths, embossing geometry PS45-5

For the first sample from above (PB600) an embossing path of 600 μm was set, for the next one 200 μm (PB200), then 400 μm (PB400). Sample “no embossing” is without embossing and the last is one with maximum embossing path until total compression (approximately 700 μm).

The different material compression of the samples within the different embossing paths is well shown. The higher the degree of embossing is, the stronger is the compression of the material. The degree of embossing is defined by the embossing path. Furthermore, not all areas within the embossing area are compressed to the same extent. The detailed thicknesses of the samples were measured with the software ImageJ.

3. Results and discussion

3.1 Material thickness initial state

The material thickness of the boards was measured. The measurement results are shown in Figure 16 on the right hand side.

3.2 Compression behavior of the paperboards

Diagram in Figure 14 shows the percentage of compressibility of the three board materials. Material A-330 shows a compressibility of nearby 57 %, materials B-325 and C-320 over 60 %. The compressibility is thus related to the material thickness. Thus, the compressibility data are comparable. The compressibility of materials B-325 and C-320 are similar, while A-330 differs significantly.

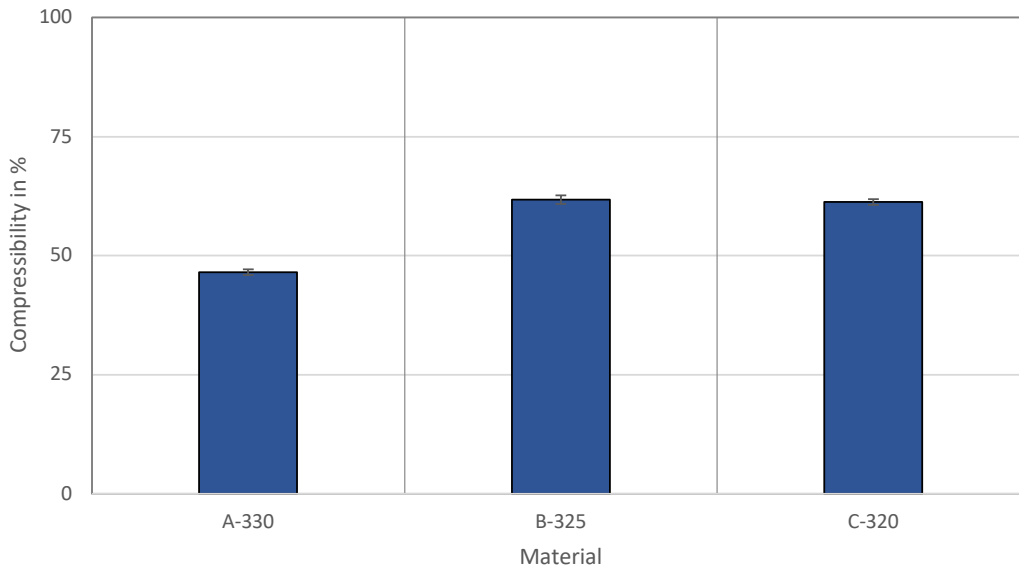


Figure 14: Comparison of compressibility of materials A-330, B-325 and C-320

3.3 Material thickness of embossed samples under pressure

Figure 15 shows the 3 materials under load at maximum compression. The material is thus compressed to the maximum. The material thicknesses in the three areas of interest are indicated in each case.

It is noticeable that the ratio between embossing path and material thickness is higher for cardboard A-330 than for the two cardboard B-325 and C-320. As shown in Figure 14, Material A-330 is less compressible. The material thickness in the flanks is higher compared to the other two materials in relation to the respective material thickness.

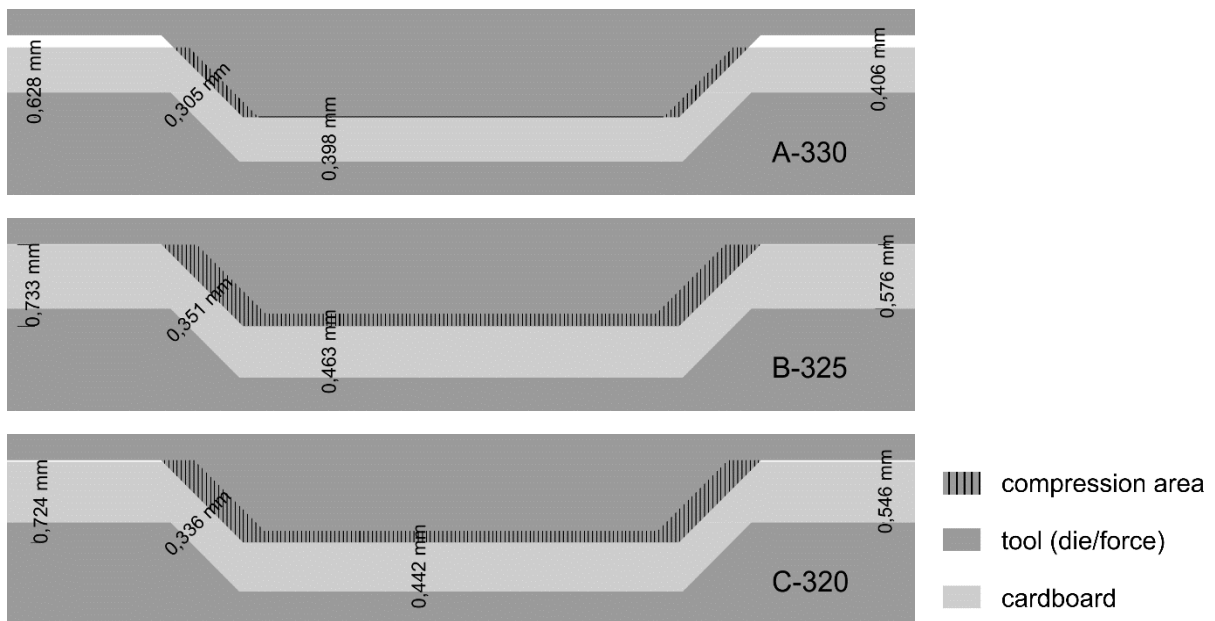


Figure 15: Effect Pairing analysis for calculating the material thickness under load for the used card materials A-330, B-325 and C-320

3.4 Re-swelling of the cardboards

It can be seen that the compressed material swells back. The depth of the indentation is thus greater in the loaded state than after load release. Figure 16 schematically shows the material behavior.

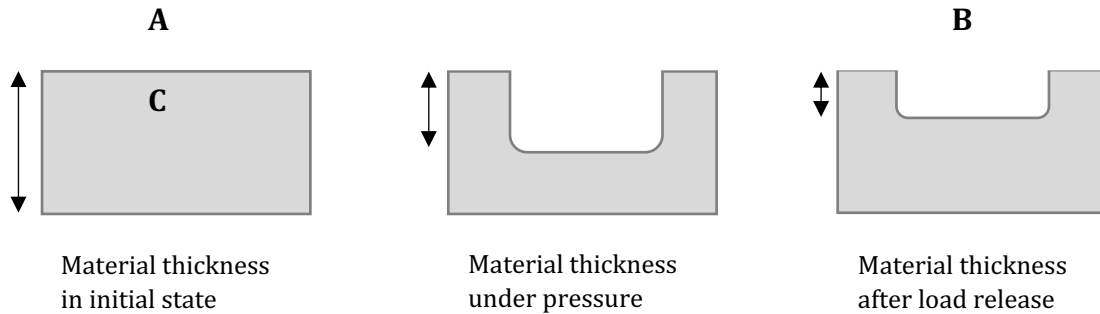


Figure 16: Material behavior re-swelling

Figure 17 shows an example of how the re-swelling affects the compression result. The compressing depth under load is significantly higher than the compression height after load release. In comparison, the resulting compression height is approximately 50 % of the compression height under load. In relation to the material thickness in the initial state, this results in a re-swelling of about 25 %.

These results show that the re-swelling has a decisive influence on the material thickness within the compression geometry. Furthermore, it influences the embossing quality, i.e. how good the impression is.

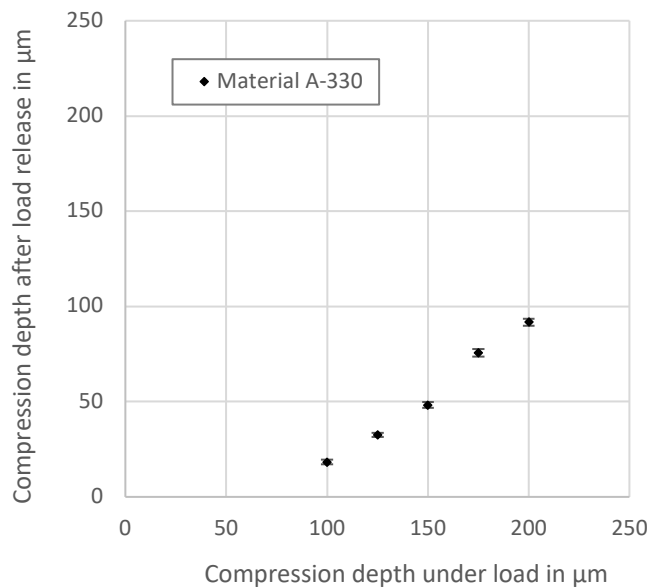


Figure 17: Comparison of the indentation depth of the compressibility stamp in the carton in the loaded state and after load release

3.5 Material thickness of the cardboard materials after load release

Figure 18 compares the different measuring methods for the material thickness in different areas of the samples after maximum compression.

It is obvious that the sample thickness on the right and left side, far off the embossing area, is the highest.

The three measurement methods *real cross section*, *virtual cross section* and *CT cross sections* show different results. It is noticeable that the material thicknesses seem to be highest for the real cross sections. The difference to the two preparation methods virtual cross-section and CT cross-section is about 100 μm . Both methods show sample thicknesses of about 400 μm . These values seem more realistic, compared with the material thickness of the material in uncompressed state (402 μm). Regarding the other areas, the material thickness measured with the CT cross section is always higher than the calculated material thickness with the virtual cross-section.

The measurement values of the real cross section and the virtual cross-section differ within factor 1.2 up to 1.5. The values in the highly compressed flanks differ even more (up to 2.0).

The CT-cross sections show that the material thickness in the area right and left beside the embossing area are uncompressed after the process. The thickness of the material is approximately 400 μm . In the middle (top of the truncated pyramid), the sample thickness is about 335 μm . Thus, in this area the material was compressed within the embossing process.

The highest compression is in the flanks of the truncated pyramid with a material thickness of approximately 250 μm .

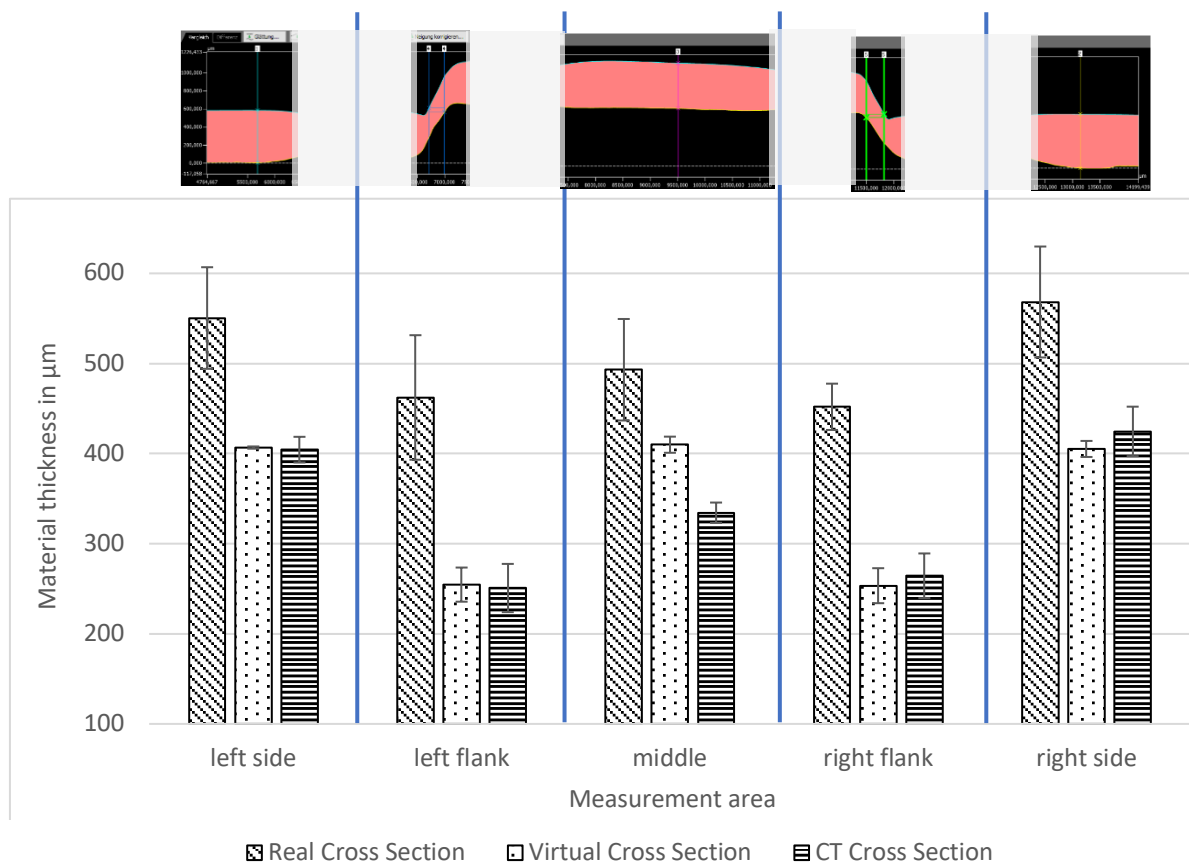


Figure 18: Comparison of the material thicknesses measured with different methods, material A-330 and assignment of the measurement data to the areas within the embossing

It can be assumed that cutting the samples physically changes the material thickness due to material damage like a delamination of the layers or the plucking of fibers. In addition, it is suspected that the cross-sectional images vary due to misplacement and mismeasurement. The images should be optimized with a modified specimen preparation and a comparative measurement procedure. Therefore, the contactless measurement methods should be preferred at the moment.

Comparing the contactless methods, the values are roughly the same. The differences between them are not significant (two sided t -test, $p = 0.975$) except in the middle of the embossing area.

Regarding results and effort, the measurement comparison has equivalent results with less effort in comparison to the CT-cross section.

3.6 Relationship compression within the compression test, compression within the embossing geometry and after load release

Figure 19 shows the material thicknesses for different loading scenarios. The material thickness in the initial state is highest at about 400 μm .

The material can be compressed to about 220 μm during compression and expands back to about 300 μm during unloading. There is thus de-compression of the material during compression.

During the embossing process, the material is also formed and compressed in the embossing nip. After unloading, the compression is also less than in the compression test alone. This suggests that tensions occur in the process that hinder perfect re-swelling. However, this would need to be investigated further.

It must always be taken into account that the forming process during coining is much more complex than when determining material compression. Energy is used not only for compression, but also for tensile and shear stresses and layer displacements. The material behavior needs to be further investigated.

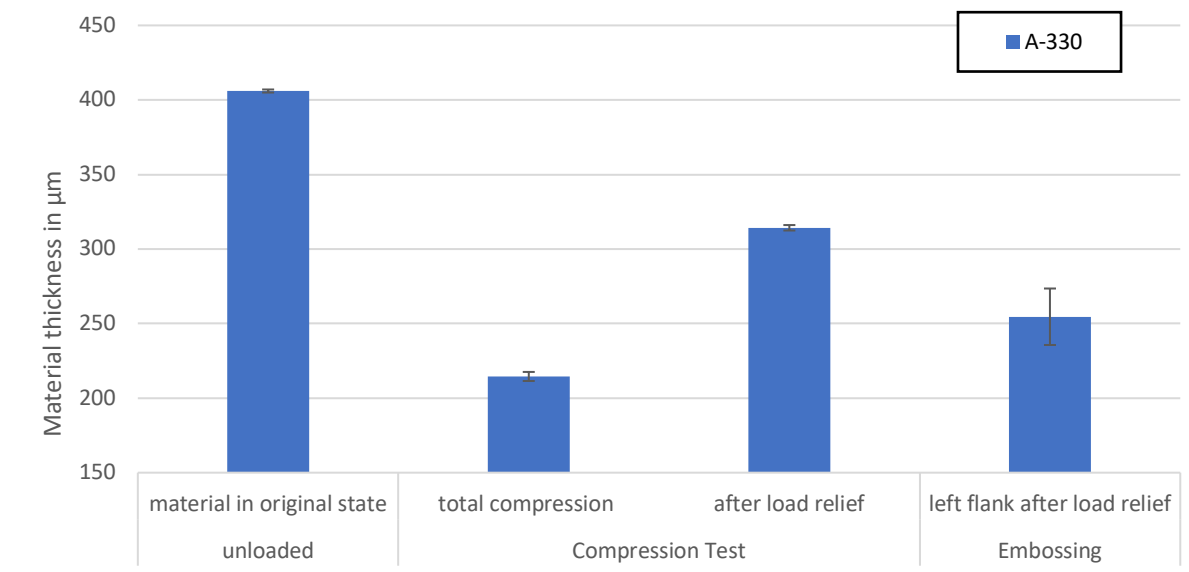


Figure 19: Comparison of the material thicknesses by different loading scenarios

4. Conclusion

The effect pairing analysis shows that compression occurs within the embossing geometry during the process. In addition, it can be seen within which partial areas compression occurs. It also allows conclusions to be drawn as to which areas are subject to particularly high or low compression.

The highest compression occurs in the area of the flanks in the case of the truncated pyramid embossing geometry.

Due to the three-dimensional forming, the virtual cross-section proved to be the most suitable substitute thickness measurement method.

The material thickness at full compression in the embossing gap and the substitute test method produce deviating results. This must be checked again.

Initial findings suggest that there tends to be less swelling back at a higher degree of forming. However, this would have to be investigated more extensively.

Acknowledgements

This work was supported by the European Social Fund and the Federal Ministry of Economic Affairs and Energy (BMWi) by funding the 100382159 research project "SmartKMU".

The authors thank Thomas Wagner of Fraunhofer IWMS for the CT-measurements.

References

- Bayerl, G. and Pichol, K., 1986. *Papier: Produkt aus Lumpen, Holz und Wasser*. Reinbek bei Hamburg: Rowohlt-Taschenbuch Verlag.
- Blechs Schmidt, J., 2013. *Taschenbuch der Papiertechnik*. 2nd ed. München: Hanser Verlag.
- Brenner, T., 2016. *Anwendung von Ultraschall zur Verbesserung der Papierfestigkeit durch Beeinflussung der Fasermorphologie*. Dresden: TU Dresden, Institut für Naturstofftechnik, Professur für Papiertechnik.
- Deutsches Institut für Normung, 2011. *DIN EN ISO 534 Papier und Pappe – Bestimmung der Dicke, der Dichte und des spezifischen Volumens (ISO 534:2011)*. Berlin: DIN.
- Ek, M., Gellerstedt, G. and Henriksson, G. eds., 2009. *Pulp and paper chemistry and technology: volume 1 – wood chemistry and wood biotechnology*. Berlin: de Gruyter.
- Hauptmann, M., 2013. *Die gezielte Prozessführung und Möglichkeiten zur Prozessüberwachung beim mehrdimensionalen Umformen von Karton durch Ziehen*. Dr.-Ing. Dissertation. Technische Universität Dresden.
- Hünniger, J., 2020. *Charakterisierung des Umformverhaltens von Karton im Reliefprägeprozess*. ZINT Doktorandenkolloquium.
- Käppeler, U., 2019 *Charakterisierung physikalisch-chemischer Veränderungen im Karton im ultraschallunterstützten Prägeprozess*. Dissertation. Hochschule für Technik, Wirtschaft und Kultur Leipzig.
- Käppeler, U., Hünniger, J., Hofmann, A., Berlich, A. and Engisch, L., 2020. Thermal influence on the mechanical properties of cardboard during an ultrasonic-assisted embossing process. *BioResources*, 15(3), pp. 5110–5121. <https://doi.org/10.15376/biores.15.3.5110-5121>.
- Käppeler, U., Schneller, K., Wallburg, F., Engisch, L. and Schoenfelder, S., 2022. (in press) Analysis of the compression behavior of different cardboard materials during embossing. In: *Tagungsband Nachwuchswissenschaftler*Innen Konferenz 2022*. Brandenburg, 11–13 May 2022. Technischen Hochschule Brandenburg.
- Meyer, M., 2015. *Entwicklung und Umsetzung eines Moduls zur Inline-Faltenauswertung an Kartonziehteilen*. Diplomarbeit. Technische Universität Dresden.
- Oehm, L., 2010. *Untersuchung des Einlaufverhaltens beim Tiefziehen von Papier und Karton*. Studienarbeit. Technische Universität Dresden.
- Radzanowski, G., 2017. *Untersuchungen zu Strukturveränderungen in Karton im ultraschallunterstützten Prägeprozess*. Master thesis. Hochschule für Technik, Wirtschaft und Kultur Leipzig.
- Schaffrath, H.-J. and Götsching, L., 1992. Modellierung der Kompression von Papier in z-Richtung bei niedriger Flächenpressung. *Das Papier*, 46(7), pp. 350–355.

Schrödel, A., 2011. Schnittherstellung mit dem Mikrotom. *Biologie in unserer Zeit*, 41(6), p. 368.
<https://doi.org/10.1002/biuz.201190099>.

Schuhmann, K., Hodes, A. and Engisch, L., 2016. Migrations- und Penetrationsprozesse im Druckprozess, Charakterisierung von Druckfarben, Papieren und Druckproben im Querschnitt. Deutsch. *Wochenblatt für Papierfabrikation – Fachzeitschrift für die Papier-, Pappen- und Zellstoffindustrie*, 30 November 2016. pp. 742–747.

Wallmeier, M., 2018. *Experimental and simulative process analysis of deep drawing of paperboard*. Dr.-Ing. Dissertation. Technische Universität Dresden.

Weber, P., 2017. *Entwicklung einer grafischen Benutzeroberfläche zur Erprobung von Wechselwirkungen zwischen den Prozessparametern des Tiefziehprozesses*. Studienarbeit. Technische Universität Dresden.